Molecular Level Stabilization of Poly(ethylene terephthalate) with Nanostructured Open Cage Trisilanolisobutyl-POSS

Flaviu Calin Ladasiu Ciolacu,[†] Namita Roy Choudhury,*[,†] Naba Dutta,[†] and Edward Kosior[‡]

ARC Special Research Centre for Particle and Material Interfaces, Ian Wark Research Institute, University of South Australia, Mawson Lakes, South Australia 5095, Australia, and NEXTEK Ltd., United Kingdom

Received May 10, 2006; Revised Manuscript Received November 5, 2006

ABSTRACT: A nanostructured organometallic macromer trisilanolisobutyl-POSS (T-POSS) was used to prevent discoloration of poly(ethylene terephthalate) (PET) and to achieve molecular level stabilization during melt processing. The resultant material was investigated using thermal analysis and oscillatory rheology. The interaction between the PET and the nanostructured additive was investigated using X-ray photoelectron spectroscopy (XPS) and matrix-assisted laser desorption/mass spectrometry (MALDI-MS). Thermal studies show that the additive increases the thermooxidative stability and consequently prevents discoloration of the material. Rheological data demonstrate increased shear storage modulus with the addition of T-POSS to PET, indicating better melt elasticity and a broader window of processability of the material. The XPS and MALDI-MS results confirm that the stabilization is achieved by covalent interaction and branching of the nanostructured additive to PET.

Introduction

Poly(ethylene terephthalate) (PET) is an important class of polymer. It is characterized by high melting temperature, excellent barrier characteristics, and mechanical properties. In many applications such as injection molding or extrusion blow molding, PET is melt processed to obtain the desired product. Such melt processing often leads to chain scission reactions due to either thermooxidative or hydrolytic attack resulting in a decrease in molecular weight and discoloration.[1,2] This also leads to loss in optical clarity of the polymer. The molecular weight loss drastically influences the processability characteristics of the polymer. This loss in average molecular weight becomes more important if the polymer is further thermally processed during recycling. Thus, stabilization against discoloration and thermooxidative degradation is of great importance to control the overall properties.[3−6]

Various types of stabilizers such as antioxidants and light stabilizers were developed to address different types of degradations. Another way to improve the stability of the polymer and increase the molecular weight during melt processing is reactive functionalization using chain extenders. Various stabilizers, chain extenders, their functions, and structures were reported in numerous works.[3−6] However, such stabilizers have a series of disadvantages limiting their inherent chemical efficiency. Stabilizers, when remain as physical mixture, can be depleted as a result of their stabilization action. Other ways of losing stabilizers are the environmental conditions in which the polymer is used. Stabilizers can be physically lost from the polymer by evaporation or leaching, and hence their concentration in the polymer decreases, leaving it susceptible to degradation.[6] Thus, there is a distinct need to develop a new type of stabilizer, which can remain in the polymer in a bound form for the lifetime of the product.

In recent years, polyhedral oligomeric silsesquioxane (POSS) is emerging as a new type of additive that offers the possibility of nanoscale reinforcement and stabilization of polymers.[7−14] Such nanosized functional materials with their high surface area and activity can lead to POSS−polymer covalent composition, remain covalently immobilized in the matrix for a prolonged period of time, and hence can limit oxidation and discoloration problems. Incorporating POSS species containing reactive groups into organic polymers creates the possibility to covalently bond the nanostructured moiety to the polymer chain, and various POSS/polymer covalent systems for different applications have been described in the literature.[7−14] In most cases, polymer reinforcement is observed to enhance mechanical and thermal properties. Also, being covalently bonded to the polymer, the loss by depletion or leaching is avoided. The multifunctional POSS macromer is an ideal additive or stabilizer for PET due to its hydroxyl and carboxyl end groups. Therefore, an open cage trifunctional POSS can react either with the hydroxyl[14] or with its carboxyl end groups, leading to branching. The decrease in acid concentration can enhance the thermal stability of the polymer[15−17] and limit discoloration.

The rheological behavior of a polymer can change during degradation due to change in molecular weight. By the addition of reactive POSS, an increase in the storage modulus and improved melt strength of the polymer could be obtained.[8] While incorporating POSS moiety into a polymer matrix results in improvements in a variety of physical and mechanical properties, the polymer can still maintain its processability characteristics.[7,8] Additionally, by controlling the degree of dispersion and limiting the degree of crystallinity,[15] the POSS-based stabilizers can also enhance the optical clarity of the polymer.

Design Rationale: It is clear that the addition of POSS-containing reactive groups can induce changes in the thermal[14] and rheological properties[8,14] of a polymer. Thus, these properties could be studied to evaluate the stabilization.[13,14,16−20] The silsesquioxane unit can be regarded as a nanaoparticle for its additive function or a well-defined macromer for its ability to undergo covalent interaction or polymerization. In this work,

[†] University of South Australia.
[‡] NEXTEK Ltd.
* Corresponding author: e-mail namita.choudhury@unisa.edu.au, Tel +61 8 8302 3719.

10.1021/ma061060d CCC: $37.00
Published on Web 12/14/2006

Scheme 1. T-POSS Structure (Top) and Possible Structures Arising from the Reaction between PET Structures and Open Cage T-POSS (Bottom)

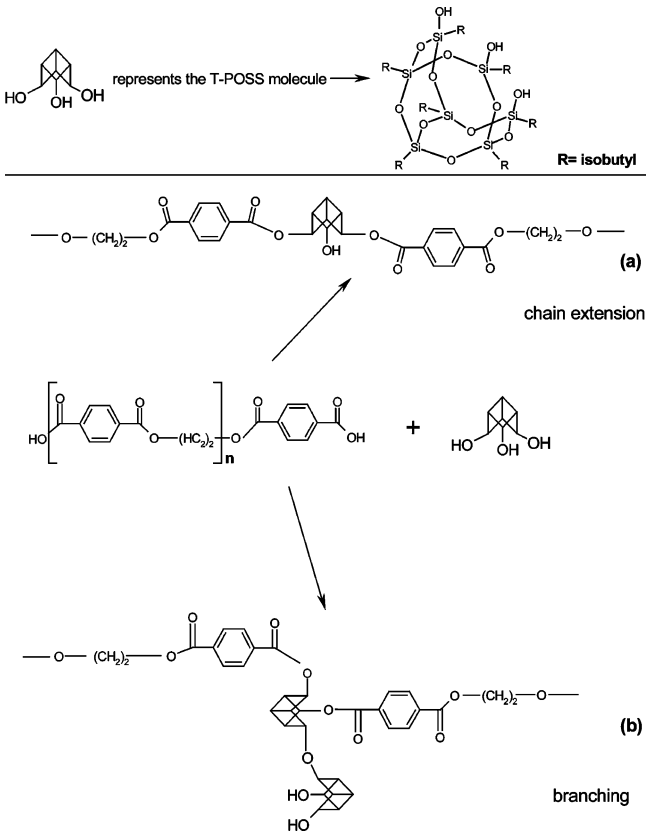

we demonstrate its use as a molecular level stabilizer resulting from polymer−cage interaction. Herein, a nanostructured open cage polyhedral oligomeric silsesquioxane (T-POSS) is used as a stabilizer for PET (Scheme 1). The hydroxyl groups of T-POSS are capable of reacting with the carboxyl end groups of PET, thus covalently binding the nanostructured moiety to the polymer. The interaction between T-POSS and PET has been monitored by X-ray photoelectron spectroscopy (XPS) and matrix-assisted laser desorption ionization mass spectroscopy (MALDI-MS). Thermal stability and processability have been examined by thermorheological measurements. The results are compared with a commercial stabilizer of synergistic combination of phosphite and hindered phenol.

Experimental Section

Materials. PET, in chips form (intrinsic viscosity 0.83 dL g^{-1}), was received from VISY Plastics Australia (Supplier SK Chemicals, Korea). Irganox B 561 was supplied by CIBA Specialty Chemical Australia and was used as a commercial stabilizer. Trisilanolisobutyl-POSS ($Si_7O_{12}C_{28}H_{66}$), henceforth referred as T-POSS, was obtained from Hybrid Plastics USA and used as received. The structure is given in Scheme 1. Trifluoroacetic acid (TFA), hexafluoro-2-propanol (HFIP), and the MALDI-MS matrix compound dihydroxybenzoic acid (DHB) were purchased from Aldrich Australia and used as received.

Sample Preparation. The PET chips were cryogenically ground to fine powder and dried for several hours at 160 °C under vacuum followed by solid phase mixing with 0.05% and 0.1% (w/w) of T-POSS. A batch with 0.2% (w/w) of Irganox B561 was also prepared in a similar way and used for comparative purposes. The mix of PET with the stabilizers was compression-molded at 280 °C for 4 min and used for thermal and rheological studies. All the samples were completely transparent, indicating uniform dispersion of the additive in PET.

Sample Preparation for MALDI-MS Analysis. 0.2 g of PET−T-POSS samples were dissolved in 1 mL of TFA, and 20 μL of polymer solution was mixed with 20 μL of DHB matrix. 1 μL of the mixture was dropped onto a stainless steel MALDI-MS plate, and the solvent was evaporated.

MALDI-MS and XPS Investigations. The nature of T-POSS/PET interaction was monitored using MALDI-MS and XPS performed on the molded polymer samples.

MALDI-TOF MS. All MALDI-MS spectra were recorded in linear mode using a Micromass M@LDI LR Instrument from Waters (UK) equipped with a pulsed (4 ns) nitrogen laser emitting at 337 nm. The detector was operated in positive ion mode, and the pulse voltage was set to 1523 V. To obtain best spectral resolution, the laser intensity was set at medium to high levels. At least 10 spectra were collected and combined.

XPS. The XPS investigation was carried out using a Kratos Axis Ultra system with monochromatic Al Kα anode (λ = 1486.69 keV). All spectra were acquired at an angle of 45°, pass energy 160 eV, and number of sweeps 2.

Thermal Analysis. The thermogravimetric analysis (TGA) was performed using a thermogravimetric analyzer (TA Instruments, model 2950) at a heating rate of 10 °C/min from room temperature to 500 °C under a controlled oxygen atmosphere. The error limit of the TGA runs was within 2%. The melting and crystallization studies were performed on a differential scanning calorimeter (DSC) (TA Instruments, DSC model 2920) with multiple heating and cooling rates of 10 °C/min under nitrogen purge.

Rheology. The melt flow behavior was studied using a TA Instruments Rheolyst rheometer (model AR 1000-N) using 2 cm parallel plates coupled with an extended temperature module. A hollow die punch was used to cut the compression-molded plaques into 20 mm diameter, 1 mm thick disks for analysis. The frequency range used was between 0.05 and 50 Hz. All experiments were run at 2 °C temperature intervals from 262 to 270 °C in air. The instrument was calibrated before every run.

Results and Discussion

Interfacial Interaction between PET and T-POSS by XPS. The PET/T-POSS material prepared by molding was examined by XPS to confirm the interaction between PET and T-POSS. Survey spectra (not presented) of virgin PET showed the presence of only carbon and oxygen, whereas for the sample of PET containing T-POSS, a small amount of silicon was also present. The binding energy and chemical composition of each element were measured. Figure 1a shows the C 1s XPS spectrum of virgin PET. This could be fitted to four peaks. The main peak at 284.7 eV (CA) is due to C−C/C−H groups from the terephthalate ring, and the other peaks at 286.4 eV (CC) and 288.6 eV (CB) are due to C−O and C═O, respectively, from the ester group. Also, a shakeup satellite peak (sh) due to the $\pi-\pi^*$ transitions in the aromatic component of PET was found at 290.9 eV. Figure 1b shows the C 1s XPS spectrum of the PET/T-POSS system. The major peak centered at 284.7 eV represents the C−C/C−H groups of PET, and the peak at 288.5 eV is due to the C═O from the ester group. The noticeable difference between the two spectra is the broadening and the shift of the peak representing the C−O bond from 286.4 eV in the spectrum of virgin PET to lower binding energy of 282.9 eV in the XPS spectrum of PET containing T-POSS (Figure 1b). The Si 2p spectra of T-POSS and PET/T-POSS are shown in Figure 1c,d. The Si 2p peak around 102 eV in the spectrum of T-POSS corresponds to the Si−O−Si bond in open cage T-POSS,[21] and the peak around 100 eV was assigned to Si−OH bond. The Si 2p peak of PET/T-POSS, however, is broader, suggesting a different chemical state of Si in the PET/T-POSS system, and also a shift to lower binding energy (99 eV) of the peak assigned to Si−OH bond was observed. Figure 1e,f shows

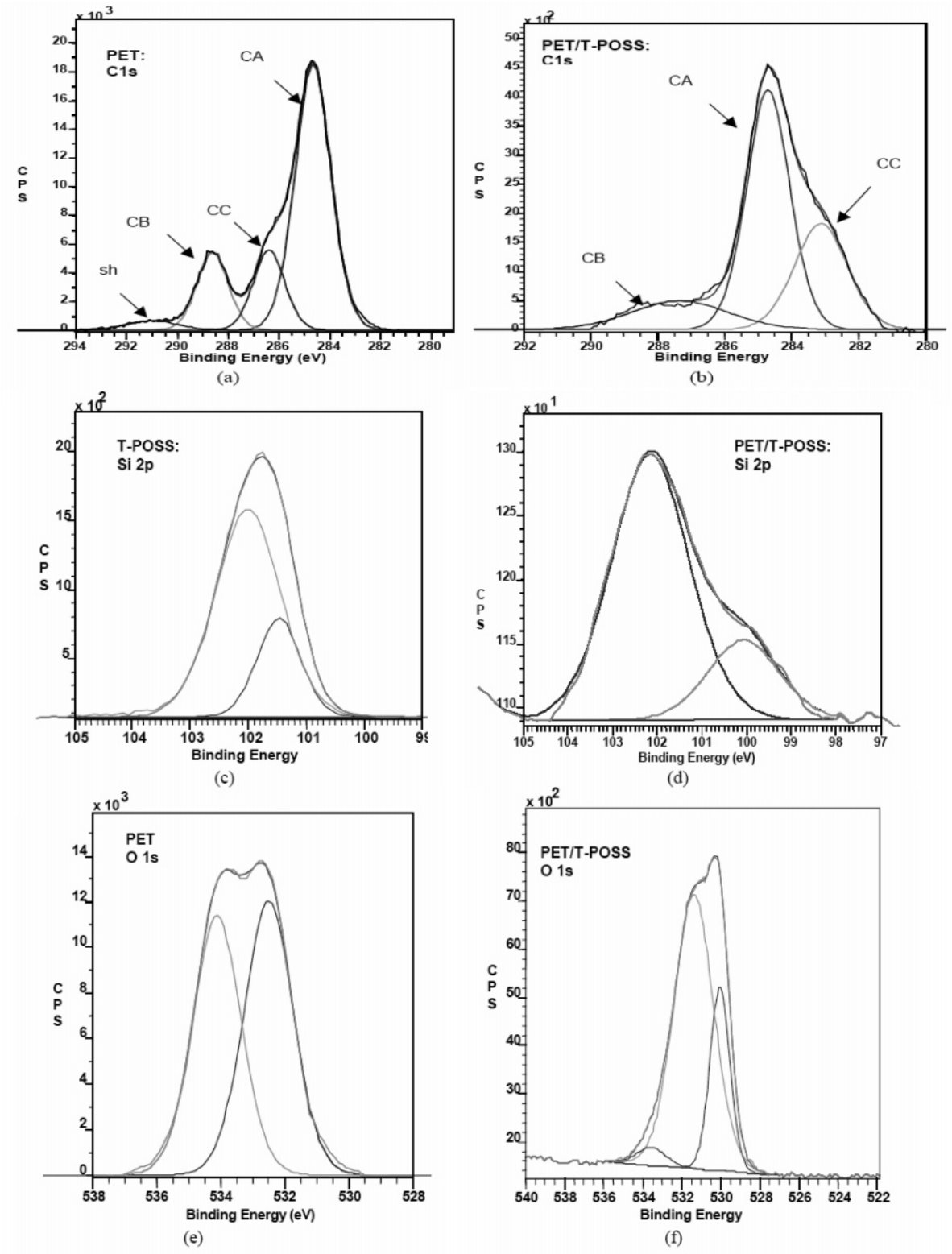

Figure 1. C 1s spectra of PET (a) and PET/T-POSS (b). Si 2p spectra of T-POSS (c) and PET/T-POSS (d). O 1s spectra of PET (e) and PET/T-POSS (f).

the O 1s spectra of PET and PET/T-POSS. The O 1s spectrum of PET could be fitted to two peaks corresponding to C−O and C═O bonds from the ester group of PET. The O 1s spectrum of PET/T-POSS, however, shows a third peak around 533 eV corresponding to the oxygen present in T-POSS.[21]

The broadening of the C 1s/Si 2p spectrum and the shift to lower binding energy of C−O bond observed in the C 1s spectrum of PET/T-POSS are ascribed to the formation of the C−O−Si bond following the reaction of the −COOH (carboxyl) end groups of PET with the −OH (hydroxyl) groups present in T-POSS (Scheme 1). The presence of a third oxygen peak from the T-POSS in the O 1s spectrum of PET/T-POSS system further supports the reaction between PET and T-POSS. The reaction with the carboxyl end groups has the advantage of reducing acid concentration, thus enhancing the thermal stability of PET during thermal processing.[17] This can also reduce or eliminate

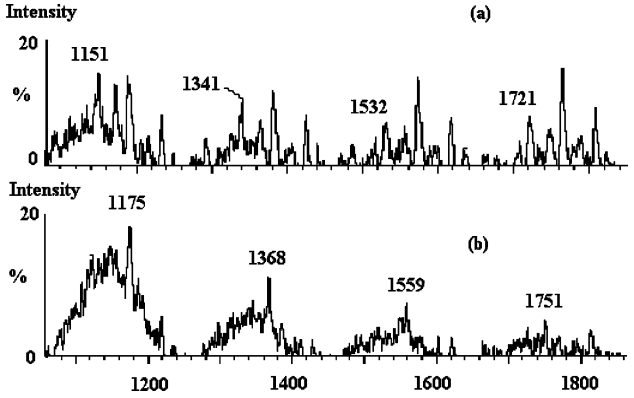

Figure 2. Enlarged sections of MALDI-MS spectra of PET and PET/T-POSS molded samples.

the yellowing of the polymer, which is partially due to the formation of additional carboxyl groups during thermal oxidation.[2]

MALDI-MS Investigation. MALDI-MS was done to investigate the reaction occurring between PET and T-POSS during molding. Figure 2a,b shows sections of the MALDI spectra of PET (a) and PET/T-POSS molded samples (b). In the MALDI-MS spectrum of the molded PET sample, the presence of linear oligomers bearing two acid end groups can be observed as seen from the peaks at *m*/*z* 1151, 1341, 1532, and 1721, together with other linear and cyclic oligomers (Figure 2a). In the spectrum of PET/T-POSS, however, the presence of such acid-terminated oligomers could not be observed, with mainly cyclic oligomers being present (peaks at *m*/*z* 1175, 1368, 1559, and 1751) (Figure 2b). The disappearance of the acid-terminated oligomers after incorporation of T-POSS strongly suggests that a reaction has occurred between the −OH groups of T-POSS and −COOH end groups from PET.

Proposed Mechanism of Interaction between T-POSS and PET. The XPS and MALDI-MS observations suggest that the T-POSS−PET interaction occurs between the −OH groups of T-POSS and −COOH end groups of PET. This can lead to macromolecular modification and consequently to reduction in acid concentration (Scheme 1a,b). However, most desirable reaction, in this case, will be star-type branching as shown in Scheme 1b, where multifunctional T-POSS can branch to more than one PET backbone. Such interaction between the polymer and T-POSS can produce significant changes in the thermal and rheological properties of the material.[8,14]

Effect of T-POSS on Thermal Properties of PET. a. TGA Investigation. In order to investigate the effect of T-POSS on PET's thermal stability and onset temperature of degradation, TGA was done both on virgin PET and on the PET samples containing the nanostructured additive, and the results were compared against the commercial stabilizer. The TGA weight loss curves of PET (P), PET/T-POSS 0.05% (PP), and PET/IRGANOX B561 0.2% (PI) are presented in Figure 3. The TG curves consist of one major decomposition step; the maximum decomposition temperatures (T_{max}) were observed at 426, 429, and 428 °C for P, PP, and PI, respectively. The onset of degradation is a clear indication of loss of thermal stability of a material. Thus, the thermal stability of the samples was evaluated from a weight loss temperature of 6%. Examination of the data clearly indicates that use of various stabilizers can enhance the thermal stability. The onset temperatures were observed at 294, 307, and 309 °C for P, PP, and PI, respectively. It is noteworthy that such stabilization is achieved using T-POSS at a level of one-fourth of that of IRGANOX B561 (0.2%).

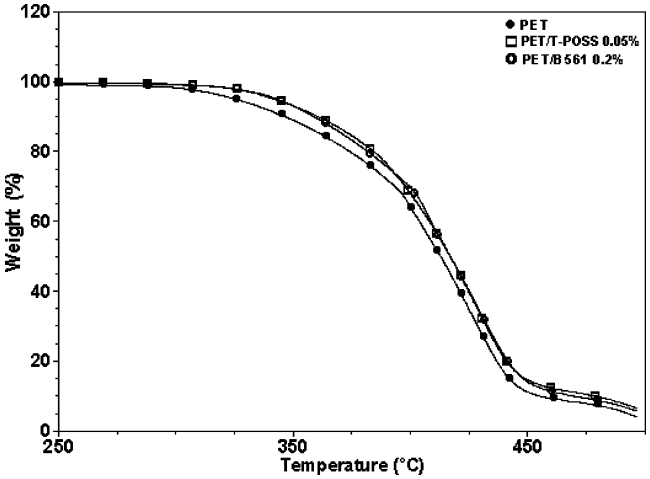

Figure 3. TGA thermograms of PET and PET with stabilizers.

The improved thermal stability can result in some form of stabilization. This can also cause retardation of the thermal inter- and intramolecular chain mobility[8] and can be seen from glass transition temperatures.[15]

In general, POSS offers higher onset of decomposition temperature to a polymer.[8] Interestingly, earlier thermal studies on PET with epoxy-POSS do not show a higher onset temperature despite the higher amount of POSS used.[14] In our work a higher onset (by 13 °C) is observed. It is important to note that to prevent any undesirable reaction of T-POSS, the polymer and the nanostructured additive were mixed in solid phase followed by molding, so that any type of chemical interaction can occur predominantly during melt processing. As the discoloration is a direct consequence of thermooxidative degradation, it is obvious that better thermal stability can offer stability toward discoloration of PET. Indeed, a visual inspection of the PET samples after the stability study over a prolonged time at 280 °C during rheology study (Figure 8) shows absence of discoloration of PET/T-POSS when compared with PET and PET with commercial stabilizer studied under same conditions.

b. DSC Investigation. Often, glass transition (T_g) and melting/crystallization temperatures (T_m/T_c) provide an in-depth understanding of the dynamics of a system. These properties are very much dependent on previous thermal history. To erase such thermal history, the samples were heated at 280 °C, kept at this temperature for 2 min, and then cooled to ambient temperature. The DSC data were collected from the second heating and cooling cycle.

Figure 4 displays the second heating and cooling curves of P and PP. The DSC data are presented in Table 1. In a total melting/cooling cycle, four distinct transitions are observed: glass transition (T_g), cold crystallization, melting of PET followed by crystallization. The glass transition temperatures (T_g) of P and PP were observed at 78 and 82 °C, respectively. It is well-known that the T_g is dependent on the molecular mobility, molecular weight, chemical structure, and other factors that influence the intermolecular forces in the polymer.[15] In the present case, although a marginal improvement in T_g is observed with only 0.05% T-POSS, yet it is believed to be the result of melt reaction of the components under shear and pressure, where miscibility of liquid−liquid interaction is possible at a molecular level. This induces changes in the chemical structure due to formation of PET/T-POSS covalent structures that hinder the mobility of the polymer chains[8] due to bulky structure of T-POSS and hence higher T_g. The reduced chain mobility affects the crystallization process increasing the amount of amorphous

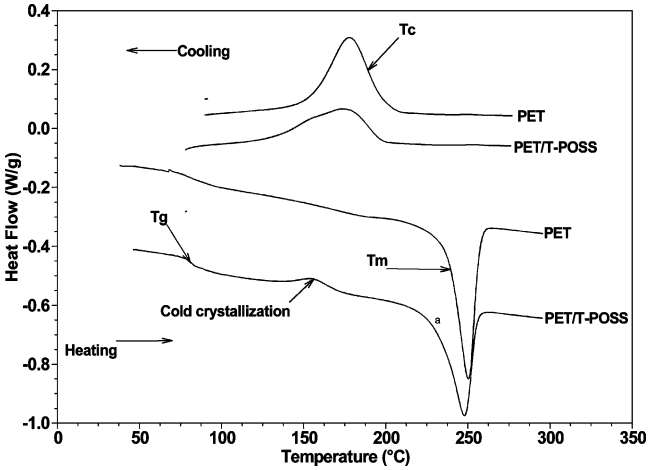

Figure 4. DSC curves of PET and PET with 0.05% T-POSS.

Table 1. Effect of Stabilizers on the Thermal Properties of PET

transitions	PET	PET/T-POSS	PET/B561
glass transition (°C)	78	82	78
cold crystallization(°C)	–	156	–
melting point(°C)	250	247	250
crystallization (°C)	178	173	178
heat of fusion (J/g)	43	37	43
deg of crystallinity (%)	31	26	31

phase in the polymer. The presence of the cold crystallization peak at 156 °C in the DSC trace of PP (Figure 4) can be clearly seen, which often takes place due to kinetic event. For P, the cold crystallization peak cannot be seen during second heating cycle, suggesting a higher amount of crystalline phase. The increased percentage of amorphous component in PET/T-POSS 0.05% is also suggested by the stronger intensity of the T_g compared to that of PET where the intensity is very weak.

The melting temperatures of P and PP were observed at 250 and 247 °C, respectively. Such melting temperature depression of PP and broadening of the melting endotherm can result only if there is any covalent attachment of the T-POSS with the PET. Yoon et al.[14] made a similar observation studying the properties of PET-containing epoxy-functionalized T-POSS. The interaction of PET with T-POSS also affects the crystallization process of the polymer during cooling. Consequently, both the degree of crystallinity and the crystallization rate of the polymer change.[15]

The effect of the nanostructured stabilizer can be clearly seen when comparing the peak associated with crystallization of P with that of PP (Figure 4). A decrease in intensity and a considerable broadening of the crystallization peak of the latter can be observed. The degree of crystallinity of P and PP has been calculated (Table 1) from the ratio of observed enthalpy to the literature enthalpy of a 100% crystalline PET (140 J g^{-1}).[22]

From Table 1 it can be seen that the percent crystallinity of PP is lower compared to that of P. The decrease in crystallinity is ascribed to the topological constraints induced by the incorporation of T-POSS. This restricts the crystallization process[15] preventing the complete packing of the polymer chains, leaving a higher amount of amorphous phase. A similar effect was observed by other authors investigating the crystallization behavior of chain extended PET.[14,19,23] Such behavior of PET (high amorphous content) is important for applications such as blow molding where optical clarity requirement is high.

The broadening of the crystallization peak is attributed to the decrease in the crystallization rate (Figure 4). It can be seen

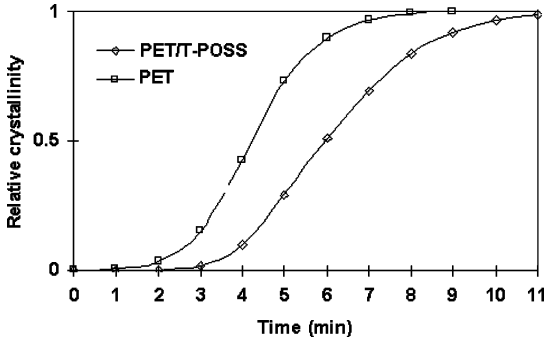

Figure 5. Crystallization curve of PET and PET with T-POSS.

from Figure 5 that the addition of T-POSS lowers the crystallization rate, and the crystallization takes place at longer times. This indicates that T-POSS is not acting as a nucleating agent to induce fast crystallization; rather, it is enhancing the melt viscosity by reactive functionalization. This is due to the fact that the diffusional motion of polymer chains from the amorphous phase to the crystalline phase is reduced by the changes in the macromolecular structure[23] following incorporation of T-POSS. As the number of heating and cooling cycles is increased, the degree of crystallinity decreases until reaches a limiting value of 26%. However, no such changes in the DSC traces of PI could be observed. In order to monitor the nature of the interaction by thermal analysis, the melt reaction was carried out using intimately mixed powders of PET and T-POSS in the same ratio (0.05% T-POSS). There was some difficulty to keep this ratio adequate. However, it was performed using more accurate balance and appropriate closure tool of the hermetic pan. Such reaction was carried out by heating the blended powders at 10 °C/min up to 280 °C and holding at this temperature for 2 min followed by cooling, and then the same cycle was repeated for second time. Further, the melt formed material was subjected to multiple DSC runs to monitor the behavior of such material.

Figure 6 a shows the two heating and cooling DSC cycles of blended PET and T-POSS powders. During the first run, the sample is mainly crystalline suggested by the low intensity of the glass transition and by the high heat of fusion of 56 J g^{-1}. During the second heating cycle, however, changes in the melting behavior can be observed. The increased intensity of the glass transition, the presence of the cold crystallization peak, and the broadening of the melting point during the second heating cycle suggest the presence of a higher amount of amorphous phase. This is also reflected by the low heat of fusion of 35 J g^{-1}. The crystallization behavior during both runs does not differ very much although a slower crystallization rate was observed during second cooling cycle. The observed changes in the melting behavior during second run clearly indicate the reactive functionalization of PET. Figure 6b shows the multiple heating and cooling DSC cycles of the melt formed PET/T-POSS system. No changes in the melting and crystallization behavior of the material can be observed even after several heating and cooling cycles. This further supports the reactive functionalization of PET and shows that the T-POSS is covalently attached to the polymer matrix.

Rheological Properties of PET/T-POSS Composite. In order to understand the stabilization effect due to mutual interaction, the melt rheological study was done on samples of PET and PET with different stabilizers in the linear viscoelastic region, over a range of temperatures and frequencies. Figure 7 shows the 3D plot of frequency dependence of the shear storage (G') modulus for PET, PET with T-POSS at different concentra-

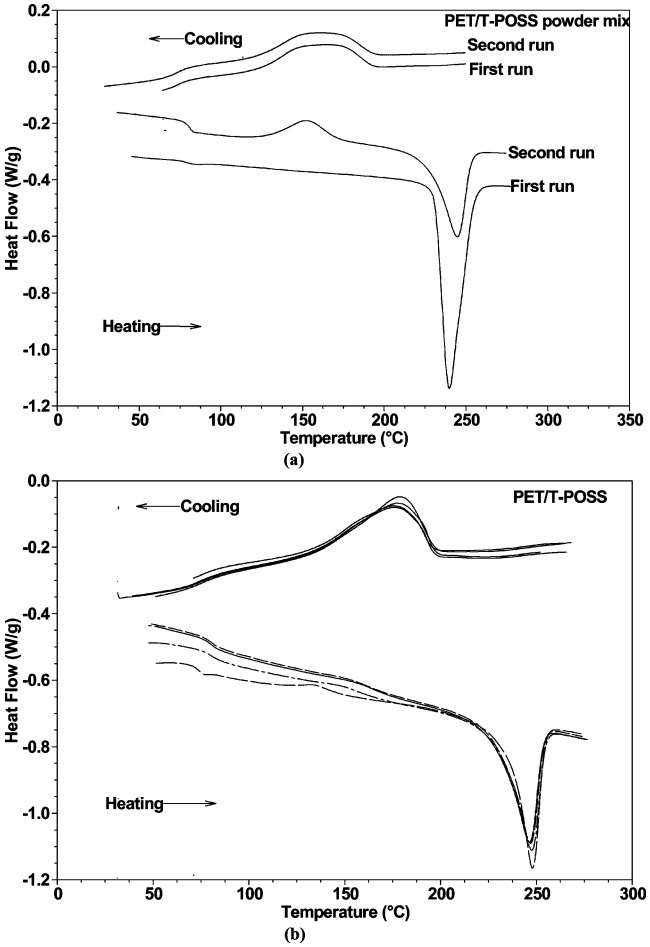

Figure 6. DSC curves of blended PET and T-POSS powders (a). Multiple heating and cooling curves of PET with T-POSS by DSC (b).

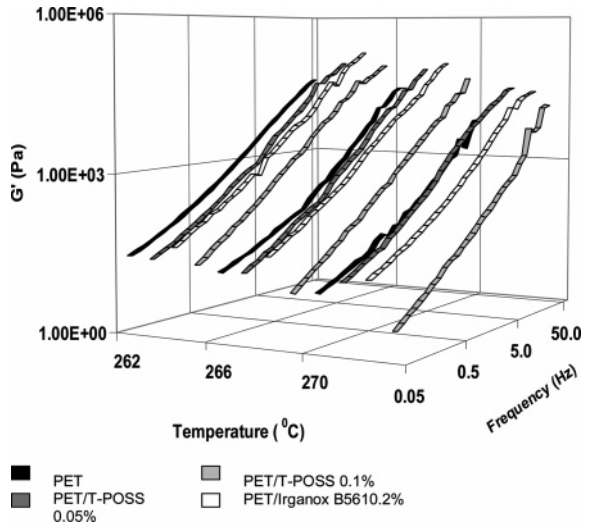

Figure 7. Shear storage (G') modulus of PET, PET with T-POSS, and PET with Irganox B561 at various frequencies and temperatures.

tions, and PET/Irganox B561 0.2% at various temperatures. It can be observed that for PET containing 0.05% and 0.1% T-POSS the G' values are higher at all temperatures than those for P and PI. Temperature dependence is less for PET containing 0.1% T-POSS. Also, the rate of increase in G' with frequency does not vary much for different samples.

Figure 8a,b shows the comparative plots of G' (a) and dynamic viscosity (η') (b) vs frequency for PET and PET with the stabilizers at 268 °C. The addition of T-POSS changes the

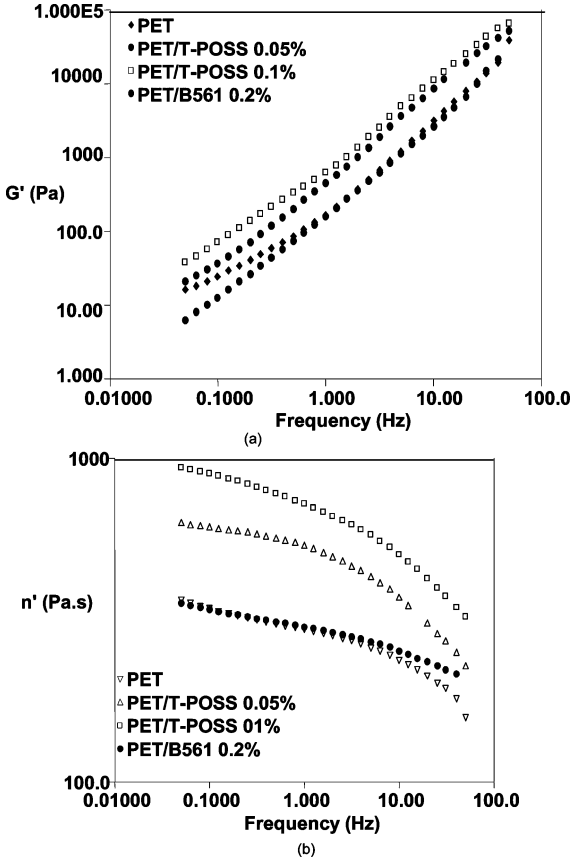

Figure 8. Shear storage modulus (G') vs frequency of PET and PET with stabilizers at 268 °C (a). Dynamic viscosity (η') vs frequency of PET and PET with stabilizers at 268 °C.

Table 2. Effect of Various Stabilizers on the Rheological Properties of PET Samples (268 °C, 1 Hz) and on the Melt Flow Activation Energy Calculated by TTS Arrhenius Modeling

sample	G' (Pa)	η' (Pa·s)	activation energy (kJ mol^{-1})
PET	163.2	295.4	167.6
PET/T-POSS 0.05%	445.2	552.5	46.3
PET/T-POSS 0.1%	603.2	693.1	58.7
PET/B561 0.2%	153.9	300.9	247.7

shear storage modulus and melt flow behavior of the polymer. Table 2 presents the G' and η' data for a frequency of 1 Hz at 268 °C. It can be seen that the G' of the polymer increases with T-POSS concentration from 163.2 Pa for PET to 603.2 Pa for PET containing 0.1% T-POSS. The addition of T-POSS also increases the dynamic viscosity of the polymer, η' being more than double (693.1 Pa·s) for PET with 0.1% T-POSS than that for PET (295.4 Pa·s) at 268 °C. However, the sample with T-POSS shows strong shear thinning behavior in the experimental frequency/temperature range.

No significant changes were observed in the G' and η' of PI at this temperature, and the same trend was observed for all the temperatures. It can be seen in Figure 8b that η' decreases with frequency. The decrease of η' occurs at lower frequencies for PET-containing T-POSS at the two concentrations compared to PET and PET containing the commercial stabilizer, showing strong non-Newtonian character of the polymer; at higher frequencies the η' values of PET and PET with T-POSS becoming convergent. It is well-known that both G' and η' depend on the overall molecular weight.[16] The higher values of G' and η', in the present case, are attributed to the chemical interaction of T-POSS with PET, leading to branching and hence resultant macromolecular modification. Such interaction influ-

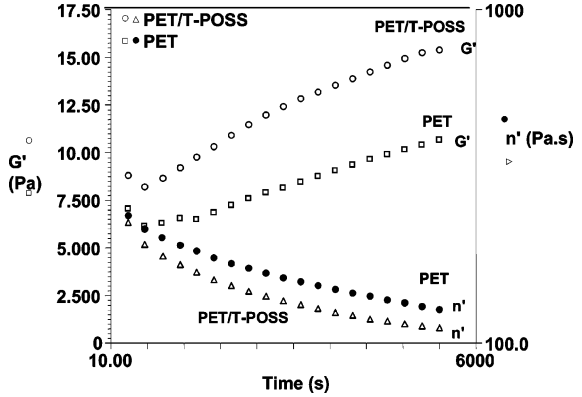

Figure 9. Time sweep experiment of PET and PET with T-POSS at 280 °C.

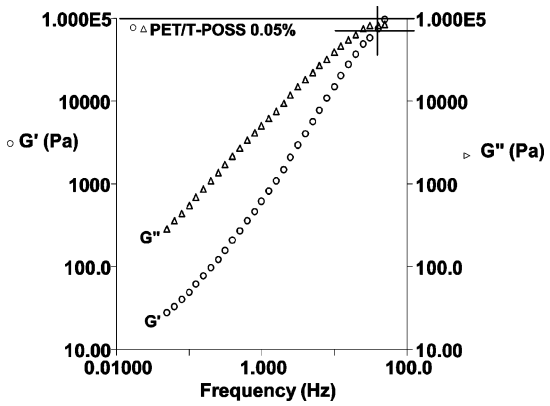

Figure 10. Frequency dependence of G' and G'' for PET with 0.05% T-POSS at 262 °C.

ences the polymer chain mobility, which is also reflected in the increased melt viscosity of the PET/T-POSS system. The increase in melt flow characteristics points to better mechanical properties and enhanced elasticity of the polymer.[16]

Figure 9 shows the G' and η' changes with time at 280 °C for P and PP. The G' increases with time for both P and PP; however, the G' of PP is at any given time almost $1^1/_2$ times higher than that of P. The η' of PP, on the other hand, is lower than η' of P. These changes in G' and η' with time of the PP system indicate higher melt elasticity, strength, and better processability of the resultant material.

Figure 10 shows the dependence of G' and the loss modulus (G'') with frequency for PP at 262 °C. It can be observed that at higher frequency the viscoelastic behavior of the sample changes with the shear storage modulus (hence elastic component as $E \propto G$) becoming predominant. The increased elasticity is important for preventing the sagging of the polymer in the mold when processed by blow molding. Moreover, the crossover point of G' and G'' for the PP system seen in Figure 10 indicates a certain degree of branching.[17] For other temperatures, G' and G'' also show a convergent behavior toward higher frequencies. However, a limited frequency range was used in this study (0.05−50 Hz) to minimize the slippage between the rheometer plates and the sample, which occurs at higher frequencies. Thus, the crossover point could not be clearly identified at those temperatures.

The convergent tendency or the crossover point of G' and G'' was not observed for virgin PET and PET with the commercial stabilizer, suggesting no change in the polymer structure and mainly viscous behavior over the entire frequency range used.

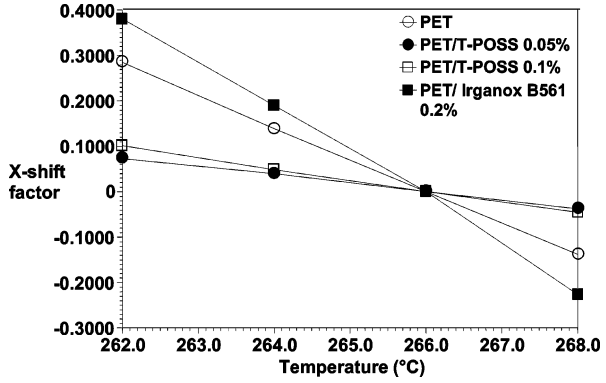

Figure 11. Plot of *x*-axis TTS shift factors (Arrhenius) against temperatures for PET alone and PET with stabilizers.

From the experimental data presented in Figure 7, it is clearly seen that G' displays similar trend for all the samples at all temperatures. Thus, the experimental data at different temperatures can be shifted along the *x*-axis into a master curve employing time−temperature superposition (TTS). This is done at temperatures above glass transition (T_g) where the Arrhenius model is applicable. The Arrhenius equation used is as follows:

$$\log aT = (-E/R)(1/T_0 - 1/T) \qquad (1)$$

where aT is the time-based shift factor, E is the activation energy, R is the gas constant, T_0 is the reference temperature, and T is the measured temperature.

Figure 11 shows the shift factor variation with temperature. Similarities can be seen in the slope of PET-containing T-POSS at the two concentrations, with PET/T-POSS 0.05% producing the lowest slope. Differences can be observed between P and PI with the latter producing the highest slope of all samples. Thus, PET-containing T-POSS displays different behavior and is less temperature dependent than PET and PET with the commercial stabilizer. By applying the Arrhenius model, the activation energy associated with the melt flow can be calculated (Table 2).

From Table 2, it can be observed that PET with T-POSS at the two concentrations exhibits lower activation energy (46.3 kJ mol^{-1} with 0.05% T-POSS and 58.7 kJ mol^{-1} with 0.1% T-POSS) than P (167.6 kJ mol^{-1}). PI shows the highest activation energy of 247.7 kJ mol^{-1} for melt flow. As the melt flow activation energy is correlated with the processability of the polymer, the low activation energy of the PET/T-POSS system indicates better processability of the polymer due to reduced polymer−polymer interaction and retention of the rheological properties over the temperature range used. Also, it broadens the processing window of these systems significantly compared to PET (as seen from temperature sensitivity of the melt viscosity) with commercial stabilizers.

Although incorporation of POSS into the polymer retards the motion, however, in many cases, it clearly acts as a flow promoter at elevated temperatures.[8] In general, melt viscosity is well correlated to the entanglement density of the polymer and hence to the degree of chain flexibility. It was reported earlier[24] that higher the temperature sensitivity of melt viscosity of a system, the higher the activation energy. Bueche[25] correlated that (melt viscosity) to the entanglement density of the polymer. Also, a large entanglement density will have less temperature sensitivity. In other words, to cause a small change in melt viscosity, a large entanglement density will require a large temperature change. It is well-known[26] that properties such as the free volume and viscosity of POSS filled copolymer can be

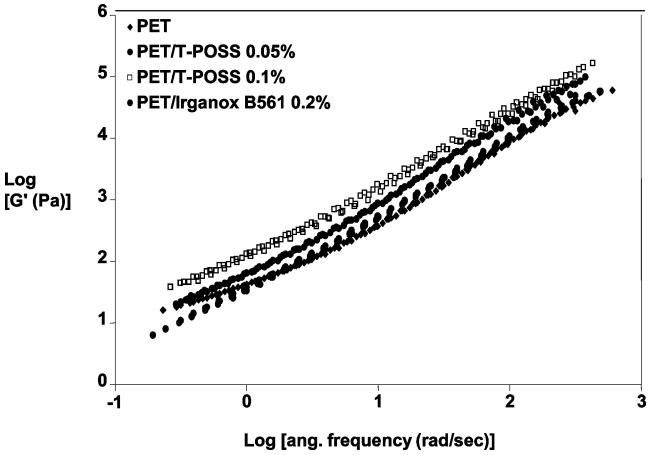

Figure 12. Master plots (Arrhenius) of storage modulus vs angular frequency for PET alone and PET with stabilizers.

manipulated by incorporating POSS in different amount. While it is reported that POSS can self-assemble,[8] in the present case the use of T-POSS distinctly changes the intrinsic characteristics of PET, which has now less crystalline component and more amorphous phase and hence free volume. In order to check the nature of interaction and whether any cross-linking has occurred, swelling studies have been done with PET/T-POSS systems at ambient temperature using TFA and HFIP. The results show that complete dissolution of the samples occurs in both solvents. This observation suggests that mainly branching has occurred.

Because of the multifunctional nature of the T-POSS, the branching is believed to be star type (Scheme 1b). The utilization of POSS as a branch point is well-known.[27] Although branched polymers are known to be rheologically complex, i.e., they do not follow a TTS, however, the TTS master plots were performed on the limited temperature and frequency ranges using all shear storage modulus data and a reference curve at 266 °C (Figure 12). Within the experimental range, the curves at different temperatures can be superimposed to one general master curve by using the shift factor concept. The plot and experimental data show good correlation and superimposability across the limited temperature ranges used.

Conclusions

The effect of open cage nanostructured T-POSS stabilizer on the properties of PET has been investigated and compared against a commercial stabilizer using thermoanalytical and spectroscopic techniques. Between the two stabilizers, the nanostructured T-POSS stabilizer improves the stability and processability of PET at significantly lower level (one-fourth of the concentration of the commercial stabilizer) due to reactive functionalization as showed by XPS and MALDI-MS investigations. The strong interaction of PET and T-POSS results in better thermal and color stability of the material. The nanostructured nature of the additive also contributes to optical clarity enhancement. The strong shear thinning behavior and decrease in melt flow activation energy of the PET/T-POSS system confirm the broader processing window of the system due to branching of T-POSS to PET. The type of stabilizer plays an important role in controlling the discoloration behavior and clarity of PET while the processability was strongly influenced by its structure and nature of interaction.

Acknowledgment. The authors acknowledge the Australian Research Council (ARC) and VISY Plastics, Australia, for the financial support of this work through a collaborative scheme. Thanks also go to Dr. N. Voelcker of Flinders University, South Australia, for his assistance in the MALDI-MS work.

References and Notes

(1) Jabbarin, S. A. Poly(ethylene terephthalate). *Polymeric Materials Encyclopedia*; CRC Press: Boca Raton, FL, 1996; Vol. 8.
(2) Ladasiu, C.; Choudhury, N. R.; Dutta, N. *Polym. Degrad. Stab.* **2006**, *91*, 875.
(3) Kelen, T. *Stabilization of Polymers; Polymer Degradation;* Van Nostrand Reinhold Co.: New York, 1983; Chapter 10.
(4) Pritchard, G. *Plastics Additives, An A-Z Reference*; Chapman & Hall: London, 1998.
(5) Brydson, J. A. *Additives for Plastics*, 6th ed.; Butterworth-Heinemann: Oxford, 1995.
(6) Pospisil, J. *Adv. Polym. Sci.* **1991**, *101*.
(7) Lichtenhan, J. D.; Schwab, J.J. *NanostructuredTM Chemicals: A New Era in Chemical Technology;* Hybrid Plastics, www.hybridplastics.com.
(8) Phillips, S. H.; Haddad, T. S.; Tomczak, S. J. *Curr. Opin. Solid State Mater. Sci.* **2004**, *8*, 21.
(9) Lee, A.; Lichtenhan, J. D. *Macromolecules* **1998**, *31*, 4970.
(10) Lee, A.; Lichtenhan, J. D. *J. Appl. Polym. Sci.* **1999**, *73*, 1993.
(11) Romo-Uribe, A.; Mather, P. T.; Haddad, T. S.; Lichtehnhan, J. D. *J. Polym. Sci., Polym. Phys.* **1998**, *36*, 1857.
(12) Fu, B. X.; Yang, L.; Somani, R. H.; Zong, S. X.; Hsiao, B. S.; Phillis, S.; Blanski, R.; Ruth, P. *J. Polym. Sci., Polym. Phys.* **2001**, *39*, 2727.
(13) Yoon, K. H.; Kumar, S.; Polk, M. B.; Min, B. G.; Schiraldi, D. A. *Polym. Prepr.* **2002**, *43*, 1283.
(14) Yoon, K. H.; Polk, M. B.; Park, J. H.; Min, B. G.; Schiraldi, D. A. *Polym. Int.* **2005**, *54*, 47.
(15) Turi, E. A. *Thermal Characterisation of Polymeric Materials*; Academic Press: New York, 1981; Vol. 1, Chapter 3.
(16) Rosu, R. F.; Shanks, R. A.; Bhattacharya, S. N. *Polym. Int.* **2000**, *49*,208.
(17) Lacoste, J. F.; Bounor-Legare, V.; Lauro, M. F.; Monnet, C.; Cassagnau, P.; Michel, A. *J. Polym. Sci., Polym. Chem.* **2005**, *43*, 2207.
(18) Dhavalikar, R.; Yamaguchi, M.; Xantos, M. *J. Polym. Sci., Polym. Chem.* **2003**, *41*, 958.
(19) Oh, S. J.; Kim, B. C. *J. Polym. Sci., Polym. Phys.* **2001**, *39*, 1027.
(20) Kang, T. K.; Kim, Y.; Ha, C. S. *J. Appl. Polym. Sci.* **1999**, *74*, 1797.
(21) Oaten, M.; Choudhury, N. R. *Macromolecules* **2005**, *38*,6392.
(22) ATHAS Database url: http://funnelweb.utcc.utk.edu/~athas/.../phenylen/pet/pet.html.
(23) Sorrentino, L.; Iannace, S.; Di Maio, E.; Acierno, D. *J. Polym. Sci., Polym. Phys.* **2005**, *43*,1966.
(24) Boudreaux, E., Jr.; Cuculo, J. *J. Appl. Polym. Sci.* **1982**, *27*, 301.
(25) Bueche, F. *Physical Properties of Polymers*; Interscience: New York, 1962.
(26) Kopesky, E. T.; Haddad, T. S.; Cohen, R. E.; Mckinley, G. H. *Macromolecules* **2004**, *37*, 8992.
(27) Bizet, S.; Galy, J.; Gerard, J.-F. *Macromolecules* **2006**, *39*, 2574.

MA061060D